ISBN: 978-3-95450-184-7 doi:10.18429/JACoW-IPAC2018-TUPML029

NOVEL PHOTOCATHODE GEOMETRY OPTIMIZATION: FIELD ENHANCING PHOTOEMISSION TIPS *

W. H. Li†, I. V. Bazarov, C. Gulliford, J. M. Maxson, Cornell University, Ithaca, NY 14853, USA

Abstract

For photoemission sources, the extraction electric field defines the maximum achievable emission current, and hence the maximum achievable beam brightness. Recently, interest has been growing in studying photocathodes with non-flat geometries to produce local field enhancements in excess of what can be achieved with large area flat cathodes. However, such geometries cause image charge effects which require self-consistent field solvers to correctly simulate. We present a novel simulation framework which combines a full particle in cell field solver (WARP) with a fast adaptive mesh space charge particle tracker (GPT) and a parallel multi-objective genetic optimizer to explore photocathode geometries for ultra high brightnesses. A first application of this technique is also shown, namely the use of field enhanced photoemission tips to create bright beams for ultra-fast electron diffraction.

INTRODUCTION

Ultrafast electron diffraction (UED) is a powerful technique that has grown in popularity for studying the structure of materials on femtosecond time scales. To push it past current spatiotemporal resolution limits, advances in the production of electron beams with higher 6D phase space density are necessary. High repetition rate accelerator-based electron sources [1, 2], often utilize bunch charges ranging from 1 to 10^6 electrons/per bunch. These electrons are typically produced from flat photocathodes, constructed from materials optimized for low intrinsic emittance, such as alkali antimonides [3]. In contrast, UED performed with modified traditional electron microscopes often utilizes non-flat, tip-based sources originally designed for field or thermionic emission. While the intrinsic emittance of these tip sources may not be optimized, the tip geometry may offer significant field enhancement.

The field enhancement generated by a tip is valuable for overcoming the virtual cathode limit [4], where the total electric field at the cathode drops below zero due to the back electric field generated by the portion of the electron beam that has already been emitted. The scaling of the space-charge limited current has been shown [5] in the cigar regime (transverse dimensions smaller than longitudinal) to be

$$I \propto (E_0 R)^{\frac{3}{2}} \tag{1}$$

where E_0 is the accelerating electric field at the cathode, and R is the initial spot size. Thus, increasing the accelerating field increases the maximum brightness achievable from the cathode [4].

Increasing the overall gun field is not often feasible, given that it is difficult to precisely control the work function across the surface of macroscopic metal electrodes, and thus performance is typically limited by field emission from localized low workfunction sites leading to vacuum breakdown [6]. However, it may be feasible to control a tip-based microscopic photocathode surface's work function, as small areas are amenable to surface science techniques such as kelvin force probe microscopy. Thus, in this work, we explore the possibility of the beam brightness gains achievable from tip based photocathodes, utilizing a novel simulation and optimization approach.

SIMULATION METHODOLOGY

These new cathode geometries require novel methods to correctly simulate. In the past, most of the simulations were done using GPT [7], a highly optimized space charge code, which is widely used in photoinjector simulations, such as [8] and [9]. Normally, the conductor geometry is fed to a separate field solver, and the resulting field maps are used by GPT to track the particles. The process is complicated by the presence of conductors while the bunch is in the proximity of the cathode. Charges near conductors create image charge effects, which cannot be pre-calculated, as they depend on the positions of each charge. Thus, they must be re-calculated at each timestep, and GPT is able to do this for flat cathodes. However, there is no ability to simulate more exotic geometries in that code.

Thus, in order to correctly simulate the particles near the cathode, a self-consistent particle tracker and field solver must be used, in our case, WARP [10]. WARP, by using a particle-in-cell Poisson solver, is able to correctly simulate the effects of image charges close to the cathode. The image charge effects are handled by re-calculating the electric field at every timestep, taking into account the positions of all charges relative to the conductors.

The methodology we developed is to run WARP while the bunch is close to the cathode and run GPT in the downstream beamline, where the image charge effects are negligible and a particle-in-cell Poisson solver is not necessary. The field is computed in the absence of charge for the interior of the gun, and slightly past the anode to avoid discontinuities in the electric field. WARP tracks the particles for several hundred timesteps, using very small timesteps during the emission process (on the order of 300 timesteps for emission), to smooth the longitudinal particle distribution. After the image charge effects become negligible, the particle positions and momenta are sent to GPT, which completes the simula-

* This work was supported by the U.S. National Science Foundation under award PHY-1549132, the Center for Bright Beams and by the U.S. Department of Energy under award DE-SC0014338.
† email: whl64@cornell.edu

ISBN: 978-3-95450-184-7 doi:10.18429/JACoW-IPAC2018-TUPML029

tion of the remainder of the beamline. The point at which the image charge effects vanish was determined by comparing the electric field at the cathode without any charge to field there at each point of the simulation. For a sense of scale, the distance that the center of the bunch has traveled when the image charge effects are less than 1% of the field is approximately 200μm for 10^6 electrons.

The cathode geometry and beamline elements were then parameterized to support the use of an optimizer. The optimizer used is the same as was used previously in [8] and [9], i.e., a multi-objective genetic algorithm.

SIMULATION RESULTS

As an example of the utility of the stitched WARP and GPT method, we consider two non-flat cathode geometries.

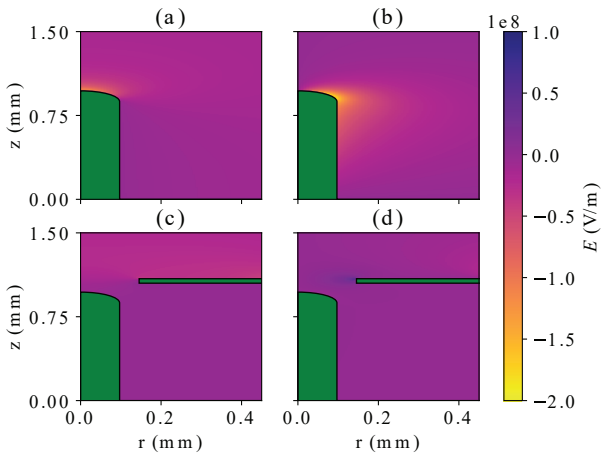

Figure 1: Field maps of the two geometries. (a) and (b) are, the longitudinal and radial electric field maps of the bare tip, respectively. (c) and (d) are the longitudinal and radial electric field maps of the tip with a Wehnelt cylinder, respectively. Of note is the strong longitudinal field enhancement caused by the bare tip, which is substantially weakened by the presence of the Wehnelt cylinder. However, the radial field maps show that the Wehnelt cylinder causes the radial fields to change from a defocusing to a focusing force.

Bare Tip

The first geometry attempted consisted of a single field-enhancing tip. A tip causes a local field enhancement roughly equal to its aspect ratio, defined as its height divided by its radius, as can be seen in Fig. 1 (a). Due to its curvature though, the tip also creates substantial radial fields away from its apex, as is seen in Fig. 1 (b). Thus, low initial emittance requires the photoemission laser spot to be much smaller than the tip, in order to avoid the aberrations caused by a quickly changing radial field [11].

The genetic optimizer was used to determine the viability of this kind of geometry. A list of the decision variables that were allowed to vary is provided in Table 1. The aspect ratio was held fixed at 10, the initial MTE was fixed at 5 MeV, and the gun used was the Cornell 225 keV cryogun. The beamline consisted of two solenoids and a 3 GHz rf buncher cavity, identical to the Eindhoven design used in [8].

Table 1: Optimizer Decision Variables (distances are with respect to previous element)

Decision variable	Min	Max
Tip radius	15 μm	100 μm
Bunch length	300 fs	20 ps
Initial spot size	1 μm	10 μm
Charge	1 fC	1 pC
Solenoid 1 peak field	0	125 mT
Solenoid 1 position	20 cm	100 cm
Buncher position	10 cm	60 cm
Buncher peak field	0	12.5 MV/m
Buncher phase	0	2 π
Solenoid 2 peak field	0	125 mT
Solenoid 2 position	10 cm	60 cm
Sample position	1 cm	10 cm

While the optimizer was running, we discovered that nearly all members of the preliminary Pareto fronts had large emittance growths down the beamline. Upon further investigation, it became clear that the issue was the extremely large divergence caused by the radial fields from the tip, caused by the very rapid change in the longitudinal E field, which, by Gauss's law, causes a large radial field. This is clearly seen in the field map in Fig. 1 (b). An example case can be seen in Fig. 2, where the red line shows the growth in beam size as a function of longitudinal position for a sample optimizer solution. The initial parameters for this case were an rms laser pulse length of 11 ps, a charge of -11 fC, an rms laser spot size of 1 μm, a tip radius of 97 μm, a tip aspect ratio of 10, and an MTE of 5 meV. The elements on the beamline are two solenoids, with a 3 GHz rf bunching cavity between them. The locations of the elements are shown above the plot. The beam size is seen to grow to over a millimeter before the solenoid begins focusing it, which leads to a geometric emittance growth of several nanometer-radians, as can be seen in [8], which is unacceptable for the purpose of preserving single-nanometer initial emittances.

Wehnelt Cylinder

A possible way to mitigate the effect of the radial fields is to introduce a Wehnelt cylinder into the cathode, which has been done in [12] and [13]. An idea of the Wehnelt cylinder geometry is given in (c) and (d) of Fig. 1. The Wehnelt cylinder is a secondary electrode near the cathode which is biased at a negative voltage relative to the cathode. This reduces the accelerating field at the cathode, but has the major advantage of reversing the radial fields from being defocusing to being focusing.

To test this, we insert a Wehnelt cylinder biased to -50 V relative to the cathode and with a tip-Wehnelt gap of 80 μm, leaving all other parameters unchanged. The effect can be seen in Fig. 2 (blue dots). The Wehnelt cylinder

ISBN: 978-3-95450-184-7 doi:10.18429/JACoW-IPAC2018-TUPML029

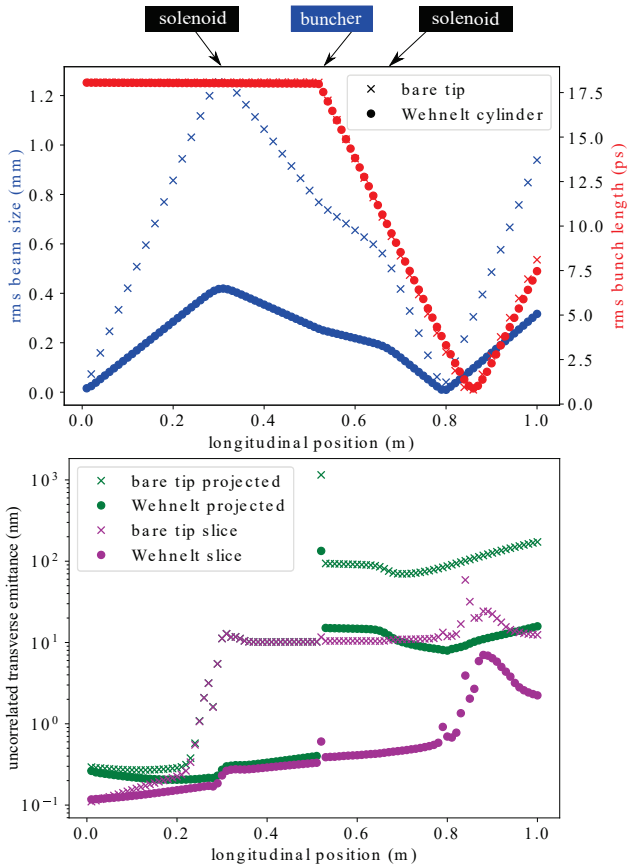

Figure 2: A comparison of the beam evolution between the bare tip and the Wehnelt cylinder. A schematic of the beamline is shown above the plots. The cathode geometry has little effect on the bunch length, but has a drastic effect on beam size and emittance. The geometric aberrations due to the first solenoid are responsible for an emittance growth of nearly an order of magnitude. The Wehnelt, by reducing the beam size growth, reduces this emittance growth enough that it is negligible. Both cases suffer a large emittance growth in the bunching cavity, but the Wehnelt shows an improvement by approximately a factor of 5. However, the slice emittances are nearly unaffected.

removes much of the defocusing at the cathode, leaving only the space charge induced divergence, which decreases the angle by a factor of 3. This causes the emittance growth from geometric solenoid aberrations to decrease by nearly two orders of magnitude, as it scales with σ^4.

The lower plot in Fig. 2 shows the emittance as a function of the longitudinal position. The rf bunching cavity drastically increases the emittance, as the head and tail of the beam experience substantially different fields. However, at all points, the beam produced by the Wehnelt cylinder has substantially lower emittance. The solenoid aberrations cannot be seen whatsoever, and, while the buncher still causes a large emittance growth, it is reduced by approximately a factor of 5 compared to the bare tip.

For comparison to the conventional projected emittance, the mean slice emittance is also plotted. This is the emittance calculated by dividing the beam longitudinally into several slices, calculating the emittance for each slice separately, and taking the mean over the slices, weighted by the number of particles in each slice. The resulting number represents the emittance neglecting misalignments caused by head-tail effects and the projection from a 6D phase space to a 4D one, thus allowing for a better look at the phase space evolution of the beam. The buncher leaves the mean slice emittance nearly unchanged for both the tip and the Wehnelt, showing that the majority of the aberrations caused by the buncher are slice misalignment effects.

It is worth noting that, in this case, we have used identical beamline parameters to the bare tip for the purposes of comparison. It is likely that the strengths of the solenoids and buncher can be optimized a great deal from this point, as they were originally optimized for the bare tip, not a cathode with a Wehnelt cylinder. This further optimization remains a work in progress. Even in this unoptimized case though, we see sub-nm slice emittance until the solenoid focus.

CONCLUSION

In these proceedings, we have shown a novel simulation methodology to handle both complex cathode geometries and downstream beamline elements. With the help of a genetic optimizer, we examined two sample cases, a bare field-enhancing tip, and a tip accompanied by a focusing Wehnelt cylinder. We found that the bare tip suffers from highly divergent fields which cause massive emittance growths due to aberrations in the beamline elements. The Wehnelt cylinder mitigates many of these problems by providing focusing immediately after the cathode, and has reduced emittances by an order of magnitude in some cases. In the future, the method outlined here can be used to examine many more exotic cathode geometries and their effects on emittance propagation.

REFERENCES

[1] D. Filippetto and H. Qian, "Design of a high-flux instrument for ultrafast electron diffraction and microscopy," *Journal of Physics B: Atomic, Molecular and Optical Physics*, vol. 49, no. 10, p. 104 003, May 2016. DOI: 10.1088/0953-4075/49/10/104003.

[2] R. K. Li and X. J. Wang, "Femtosecond MeV Electron Energy-Loss Spectroscopy," *Physical Review Applied*, vol. 8, no. 5, p. 054 017, Nov. 2017. DOI: 10.1103/PhysRevApplied.8.054017.

[3] I. Bazarov *et al.*, "Thermal emittance measurements of a cesium potassium antimonide photocathode," *Applied Physics Letters*, vol. 98, no. 22, p. 224 101, May 2011. DOI: 10.1063/1.3596450.

ISBN: 978-3-95450-184-7 doi:10.18429/JACoW-IPAC2018-TUPML029

[4] I. V. Bazarov, B. M. Dunham, and C. K. Sinclair, "Maximum achievable beam brightness from photoinjectors," *Physical Review Letters*, vol. 102, no. 10, 2009. DOI: 10.1103/PhysRevLett.102.104801.

[5] D. Filippetto, P. Musumeci, M. Zolotorev, and G. Stupakov, "Maximum current density and beam brightness achievable by laser-driven electron sources," *Physical Review Special Topics - Accelerators and Beams*, vol. 17, no. 2, p. 024 201, Feb. 2014. DOI: 10.1103/PhysRevSTAB.17.024201.

[6] P. G. Slade, *The vacuum interrupter : theory, design, and application*. CRC Press, 2008, ISBN: 9780849390913.

[7] *Pulsar Physics GPT*. http://www.pulsar.nl/gpt

[8] C. Gulliford, A. Bartnik, and I. Bazarov, "Multiobjective optimizations of a novel cryocooled dc gun based ultrafast electron diffraction beam line," *Physical Review Accelerators and Beams*, vol. 19, no. 9, 2016, ISSN: 24699888. DOI: 10.1103/PhysRevAccelBeams.19.093402.

[9] I. V. Bazarov, A. Kim, M. N. Lakshmanan, and J. M. Maxson, "Comparison of dc and superconducting rf photoemission guns for high brightness high average current beam production," *Physical Review Special Topics - Accelerators and Beams*, vol. 14, no. 7, p. 072 001, Jul. 2011. DOI: 10.1103/PhysRevSTAB.14.072001.

[10] A. Friedman *et al.*, "Computational methods in the warp code framework for kinetic simulations of particle beams and plasmas," *IEEE Transactions on Plasma Science*, vol. 42, no. 5, pp. 1321–1334, 2014, ISSN: 00933813. DOI: 10.1109/TPS.2014.2308546.

[11] J. Maxson, C. Gulliford, I. Bazarov, L. Cultrera, H. K. Fung, and H. Lee, "Single photoemitter tips in a dc gun: Limiting aberration-induced emittance," in *Proc. 8th Int. Particle Accelerator Conf. (IPAC '17)*, Copenhagen, Denmark, May 2017, paper TUPAB128, pp. 1622–1625.

[12] S. Ji *et al.*, "Influence of cathode geometry on electron dynamics in an ultrafast electron microscope," *Structural Dynamics*, vol. 4, no. 5, 2017. DOI: 10.1063/1.4994004.

[13] K. Bücker *et al.*, "Electron beam dynamics in an ultrafast transmission electron microscope with Wehnelt electrode," *Ultramicroscopy*, vol. 171, pp. 8–18, Dec. 2016. DOI: 10.1016/j.ultramic.2016.08.014.